

- 38 (a) A shallow layer of warm water near the sea surface can develop, which
 39 makes the SST not representative of the bulk of the mixed layer of the
 40 ocean (e.g., Katsaros et al., 1983; Stramma et al., 1986; Soloviev and
 41 Lukas, 1997; Gentemann et al., 2003; Stuart-Menteth et al., 2003).
- 42 (b) In addition, if horizontal temperature gradients exist in the surface water,
 43 the simultaneous cooling from the sea surface by evaporation, sensible
 44 heat loss, and longwave radiation would be larger from the warmer water
 45 than from the cooler side of the gradient associated with features such as
 46 fronts or eddies, leading to greater net heating on the cool side. This
 47 results in a reduction in the horizontal temperature gradients and erro-
 48 neous inferences about the mixed layer (Katsaros and Soloviev, 2004),
 49 which may have consequences for fishing and other activities.

50 The analysis presented herein includes an additional regulating feedback
 51 via a dependence of the wind stress on atmospheric stability. We illustrate the
 52 effect of a reduction in the SST horizontal gradients with model calculations
 53 and with observations from a mooring array deployed on the shelf off south-
 54 east Florida. This mooring array is primarily intended for monitoring the
 55 coastal circulation and environmental conditions (Soloviev et al., 2003a, b).

56 For this study we assume that the air is modified through a deep layer and
 57 is relatively well mixed as it flows across the SST gradient (therefore the
 58 difference in the overlying air is not great from the warm to the cold SST).
 59 Other situations, even such where a mesoscale circulation (analogous to a sea
 60 breeze) develops between warm and cold water areas (Mahrt et al., 2004),
 61 can occur. We are not focusing on such cases herein, and are, in fact, dis-
 62 cussing only a fraction of possible scenarios.

2. Background

64 The equations for heat, salinity and momentum balance for the upper layers
 65 of the ocean are defined in a companion paper (Katsaros and Soloviev, 2004).
 66 We will not repeat the development here, but only summarize the procedure.
 67 The time dependent equations for the vertical diffusion of heat, salt and
 68 the two components of horizontal momentum are solved iteratively, with the
 69 turbulent exchange coefficients of these properties being dependent on the
 70 gradient Richardson number, which depends on all three variables sought.
 71 The surface boundary conditions are the net heat flux due to the three loss
 72 terms: latent heat flux, sensible heat flux and net longwave radiative heat loss
 73 to the atmosphere and space; the salt flux into the sea as a consequence of the
 74 evaporation; and the two components of the wind stress on the sea surface
 75 due to atmospheric forcing. The surface fluxes are determined from the
 76 Tropical Ocean Global Atmosphere–Coupled Ocean Atmospheric Response

77 Experiment bulk formulation (TOGA-COARE 2.6 algorithm, Bradley et al.,
 78 2000). Solar radiation is treated as a volume source of heat for the ocean. We
 79 assume clear skies and that the near surface atmosphere has the same air
 80 temperature, water vapour content and mean wind speed over the whole
 81 region. The grid used has 40 evenly spaced grid points for the top 10 m of the
 82 sea, and a small constant vertical velocity gradient ($2 \times 10^{-4} \text{ s}^{-1}$) is assumed
 83 to avoid extremes in the Richardson number in the first time step. (Katsaros
 84 and Soloviev, 2004).

85 Aspects of this calculation for low-latitude, warm water cases are pre-
 86 sented in Figures 1 and 2. Note that there is almost three times as much heat
 87 input from the sun as the heat loss due to the turbulence and longwave
 88 radiation terms over a 24-h period (Figures 1a and c). This allows us to draw
 89 general conclusions even if we do not simulate the fluxes exactly, and even if

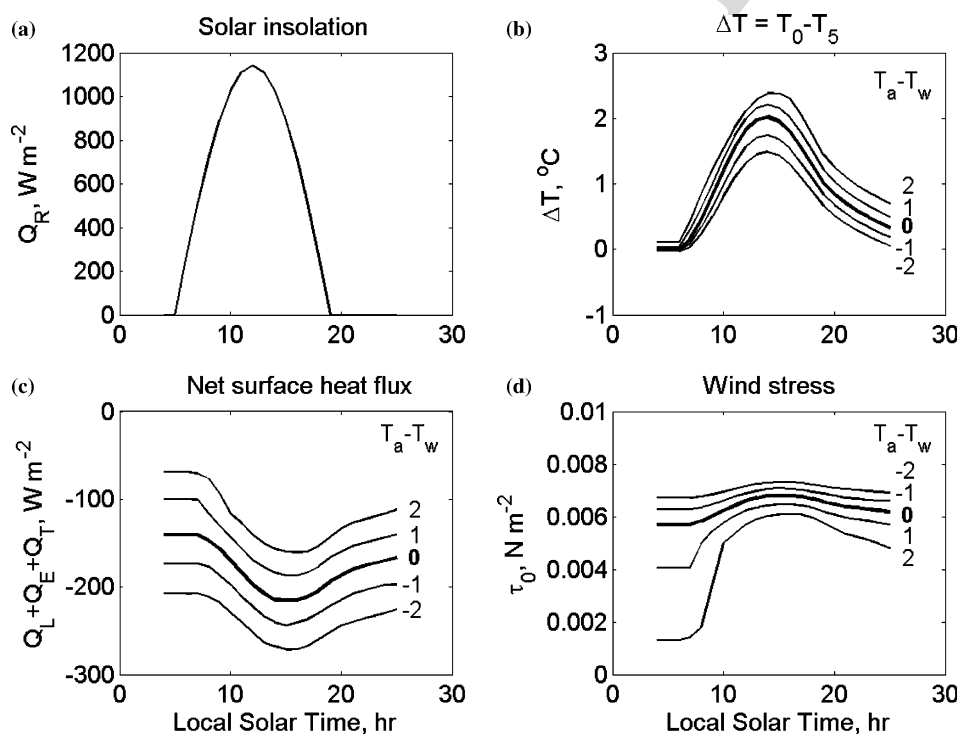


Figure 1. Modelling the effect on SST due to atmospheric regulation. Modeling parameters are representative of the calculated Straits of Florida cases, wind speed 2 m s^{-1} , specific humidity 16 g kg^{-1} , and air temperature $28 \text{ }^\circ\text{C}$. (a) March of the insolation rate, (b) model calculation of the temperature difference between the sea surface (T_0) and 5 m depth (T_5) over 22 h of time, (c) the associated values of the net heat loss term and (d) wind stress change. The symbols in (c) represent the following: Q_T , sensible heat loss, Q_E , longwave and Q_L , latent heat loss. The curves in the plot are labeled with the difference between the initial water temperature, T_w , and the fixed air temperature, T_a .

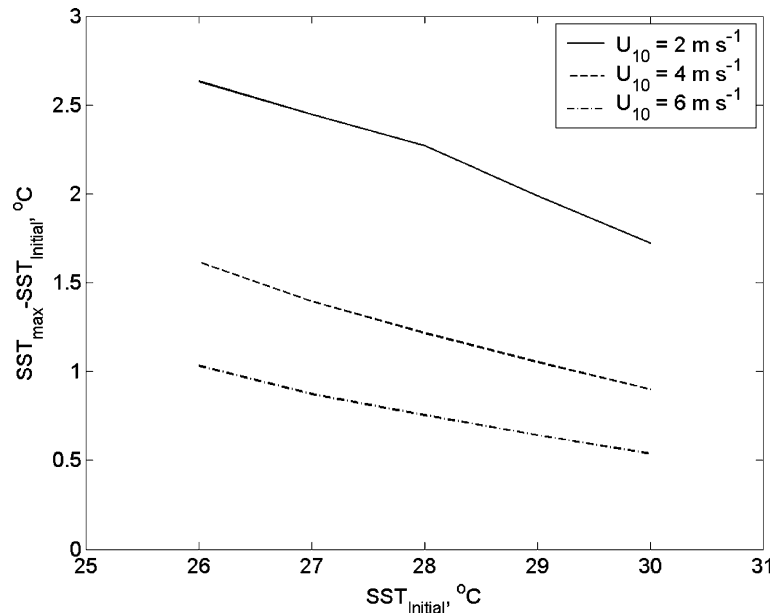


Figure 2. Dependence of the change in SST on the initial water temperature. Modeling parameters are representative of the Gulf of Mexico and the Florida Straits cases, wind speed at a 10-m height from 2 to 6 m s⁻¹, specific humidity 16 g kg⁻¹, and air temperature 28 °C.

90 the atmospheric temperature and humidity would be somewhat different over
 91 the warmer and colder areas during the day. However, even with weak winds,
 92 the air flows rapidly across these temperature variations in the water and the
 93 atmosphere tends to be well mixed through a rather deep layer if there is
 94 unstable stratification.

95 Figure 1b shows that the diurnal warming peaks shortly after maximum
 96 insolation and before the heat-loss-driven convective motions in the ocean
 97 generate a new near-surface mixed layer. Figure 1d demonstrates the
 98 dependence of the wind stress on the march of the heat fluxes. Initially, the
 99 wind stress on the sea surface is reduced for the two cases when the water
 100 temperature (T_w) is below the air temperature (T_a) ($T_a - T_w = 2$ °C), hence
 101 stable stratification in the atmospheric surface layer. Lower wind stress leads
 102 to a higher diurnal warming rate because of reduced mixing in the near-
 103 surface layer of the ocean. The SST reaches the value of the air temperature
 104 around 1000 local standard time (LST) and the surface wind stress increases
 105 due to increased mixing in the atmospheric boundary layer. The air-sea ex-
 106 change coefficients for momentum, heat and water vapour all increase rapidly
 107 at this time.

108 Our example in Figure 1 gives just one possible scenario, but a typical one
 109 for the Straits of Florida region and a wind speed of 2 m s⁻¹. Figure 2

110 illustrates the consequences for the SST for the same range in initial water
111 temperatures and the same atmospheric fixed conditions as seen in Figure 1.
112 It also includes plots for the same initial water temperatures and atmospheric
113 conditions, but with greater wind speeds. Even at a mean wind speed of
114 6 m s^{-1} at 10-m height substantial warming occurs at the surface during
115 maximum solar radiation. Many other combinations of the input variables
116 will occur in a given month and particularly over the course of a year, but
117 these calculated values are representative of the diurnal heating process,
118 which leads to a weakening of horizontal temperature gradients.

119 Figure 2 also illustrates what happens to the temperature difference, ΔT ,
120 between the initial temperature of the well-mixed upper ocean and the top-
121 most grid point of our calculation at 0.25 m, after the diurnal heating cycle
122 under low wind speed conditions. The ΔT is largest in the initially colder water
123 (illustrated by the negative slope of the curve) by an amount that depends on
124 the mean wind speed, all other factors remaining equal. This suggests that, if a
125 front exists in the water, the surface-temperature gradient is reduced after
126 such a day, masking the front from a remote sensing perspective.

3. Experimental Evidence

128 3.1. DESCRIPTION OF THE FIELD SITE

129 As a part of the South Florida Ocean Measurement Center (SFOMC),
130 NOVA Southeastern University (NSU) and the University of South Florida
131 (USF) deployed a three-dimensional mooring array with acoustic Doppler
132 current profilers (ADCPs) and a combination of inductively coupled and/or
133 self-recording temperature/salinity and pressure sensors. The NSU/USF
134 observations were coordinated with the University of Miami Ocean Surface
135 Current Radar (OSCR) deployments. The bottom instruments work in a self-
136 recording mode, while the surface moorings transmit real time data via
137 spread-spectrum radio. The surface moorings are monitored through
138 the ARGOS satellite network. Figure 3 shows the mechanical construction of
139 the C-buoy and an overview of the location of the field measurements on the
140 south-east Florida shelf.

141 Measurements collected at the sites relevant to our study are from MicroCat
142 SBE-37SM instruments measuring, every 30 min, sea temperature and con-
143 ductivity at 0.5, 5, 10, and 15 m on the C-buoy and meteorological variables
144 collected by a coastal climate weather package on the same buoy. (The pre-
145 cision of the temperature sensor on SBE-37SM is better than $0.002 \text{ }^\circ\text{C}$). The
146 meteorological variables include, wind speed and direction, surface pressure,
147 air and near-surface water temperature, relative humidity, solar radiation,
148 longwave radiation and the cumulative rainfall (measured every 5 min).

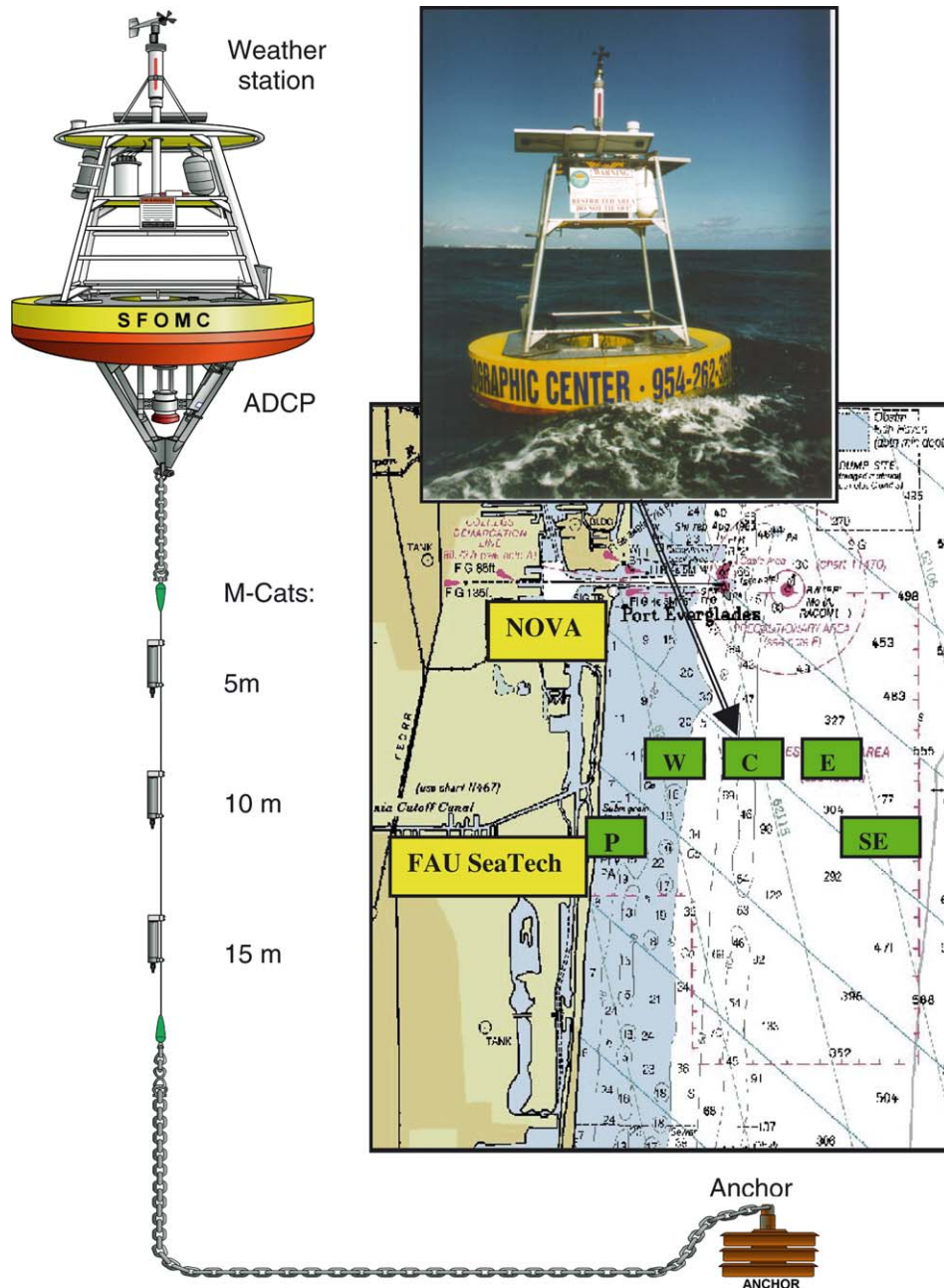


Figure 3. Design of surface mooring C and overview of the measurement site during the Year 2000 experiment. W is the west (bottom) mooring (at 11 m isobath), C is the central mooring (at the 20 m isobath), and E is the east mooring (at 50 m isobath). SE is the University of Miami acoustic mooring and P is the Dania Pier meteorological station. Observations from mooring C are used herein.

149 3.2. DATA USED

150 Figure 4 gives a time series of the upper ocean temperature evolution at two
 151 depths and the nearby meteorological measurements for June 2–27, 2000,

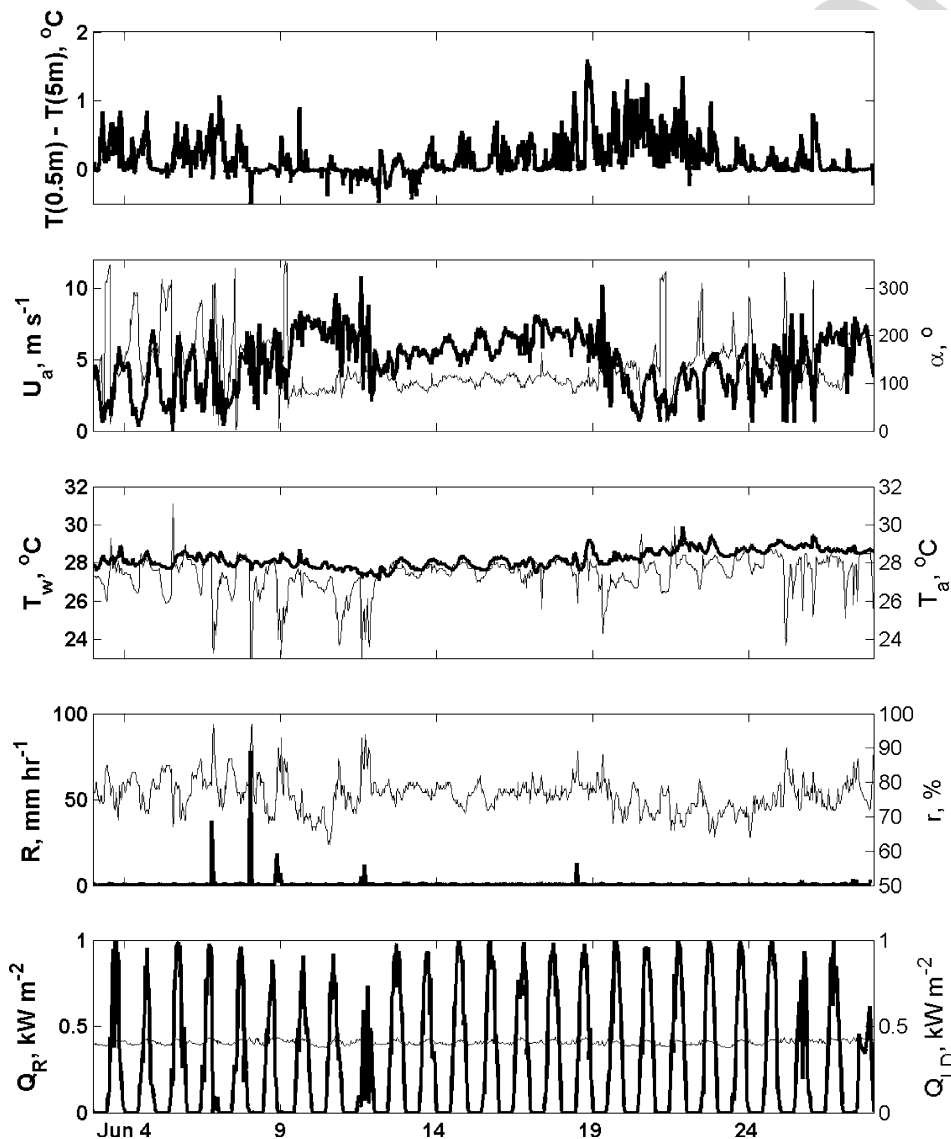


Figure 4. Hydro-meteorological conditions during the June 2000 experiment on the shelf of south-east Florida: (a) temperature difference between 0.5 and 5 m depth; (b) wind speed U_a (bold line) and wind direction α ; (c) water temperature T_w (bold line) and air temperature T_a ; (d) rain rate R (bold line) and relative humidity r ; (e) shortwave solar radiation Q_R (bold line) and downwelling longwave radiation Q_{LD} .

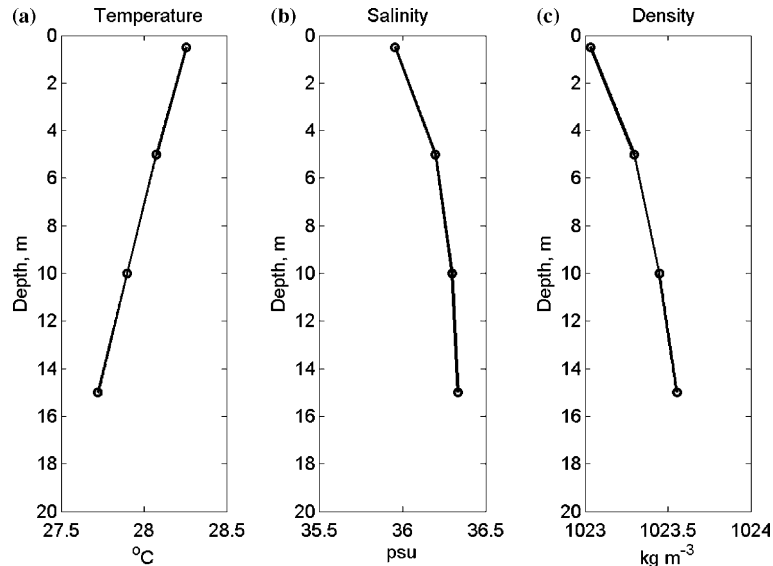


Figure 5. Vertical temperature, salinity, and density profiles at the C-mooring location averaged over a 25-day period.

152 sampled every 30 min. Figure 5 shows the vertical temperature, salinity and
 153 density profiles at the C-mooring location averaged over the 25 days, dem-
 154 onstrating the thermal stratification that was present. We have selected this
 155 period for analysis because of the prolonged interval of low wind speeds in
 156 the middle of the month.

157 3.3. RESULT FROM FLORIDA STRAITS

158 Figure 6a shows a plot of ΔT in the water calculated as the difference between
 159 the 0.5 and 5 m measurements. The data are from the same period as in
 160 Figure 4. They represent data for all 25 days, night time as well as daytime,
 161 using the following selection criteria:

- 162 (1) Salinity difference in the upper 5 m less than 0.5 psu (practical salinity
 163 units).
 164 (2) The wind speed less than 4 m s^{-1} .

165 The first criterion was chosen to eliminate cases with strong precipitation
 166 effects, while the second criterion was applied to isolate conditions of low
 167 wind speed.

168 After applying these selection criteria, a total of 311 points remained, see
 169 Figure 6a, where we see the tendency for the points to follow a declining slope

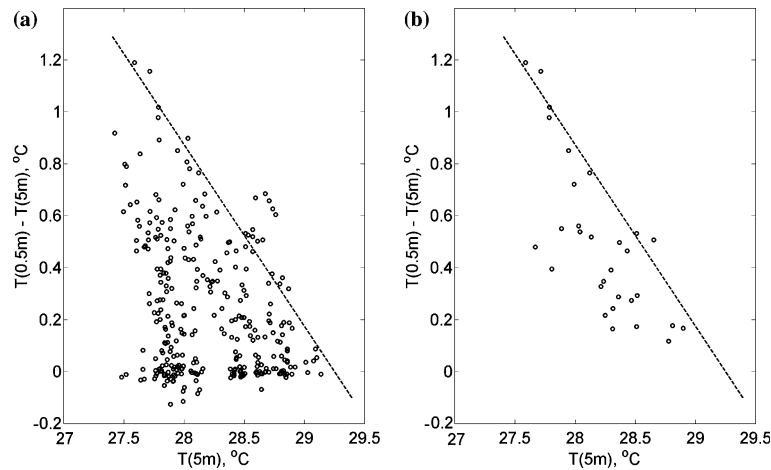


Figure 6. (a) Dependence of the temperature difference, ΔT , between 0.5 and 5 m on the temperature at 5 m depth for 25 days in June 2000 under conditions of no rain and wind speed $< 4 \text{ m s}^{-1}$. (b) Same as in subplot (a) but only from 1100 through 1700 LST, and for $T_w - T_a < 1.5 \text{ }^\circ\text{C}$.

170 as in the simulation of Section 2 (Figure 2) with the largest ΔT occurring in
 171 the colder water. In this case there are many points in the triangle below the
 172 line of the maximum temperature difference. These points represent times
 173 before and after maximum ΔT . There are also many points on the line at zero
 174 values of ΔT , which corresponds to periods with strong mixing due to con-
 175 vective cooling when no diurnal layer of warm water is formed.

176 Diurnal warming could penetrate down to 5 m, so ΔT may not necessarily
 177 represent the full diurnal warming. The exponential decay of solar radiation
 178 in sea water allows some radiation to be absorbed below the 5 m depth and
 179 some heat can be transported to this depth by turbulence. The overall effect
 180 of diurnal warming on the water temperature below 5-m depth is relatively
 181 small. In order to make our model and measurement results comparable, the
 182 model results shown in Figure 2 are given for the same depth range as given
 183 by the data in Figure 6. The temperature difference between 0.5 and 5 m
 184 could occasionally be affected by sub-mesoscale eddies and/or baroclinic
 185 tides, which are strong in this area (Soloviev et al., 2003a, b).

186 In order to select the cases with a developed diurnal thermocline, an
 187 additional, third criterion has been applied for data selection:

188 (3) Daytime hours from 1100 through 1700 LST and conditions of the
 189 water-air temperature difference, $T_w - T_a < 1.5 \text{ }^\circ\text{C}$, have been chosen.

190 After applying selection criteria 1, 2 and 3, a total of 30 points remained
 191 (Figure 6b). The remaining points are less scattered than those in Figure 6a,
 192 since the cases of strong convective cooling (nighttime or large water-air
 193 temperature differences) have been filtered out. The water column was

194 stratified during this observational period as seen in Figure 5. As a result, the
 195 bottom and surface boundary layers were not overlapping. This ensured that
 196 the diurnal cycle of solar radiation, rather than barotropic tidal motions, was
 197 the main cause of the observed variability of SST.

4. Discussion

199 The calculation of the exact amount of increase in SST over a 24-h period,
 200 and the associated reduction in SST gradients in any particular situation,
 201 must be performed with the appropriate upper-ocean mixing, the complete
 202 stratification effects and variations in the atmospheric fluxes, for air flowing
 203 from warm to cold, cold to warm water, or parallel to the SST gradients. Any
 204 advection in the water should also be accounted for, although it is typically
 205 not very large over a 1-day period. Our case is not the most extreme, since
 206 Gentemann et al. (2003) and Stuart-Menteth et al. (2003) in extensive anal-
 207 yses of satellite data reported even larger day-to-night SST differences.

208 This example is only indicative of the situations that one would encounter
 209 in summer-time at low latitudes, whenever the wind speed is relatively weak
 210 and the diurnal heat fluxes result in net heating. Our most important result
 211 and that of Katsaros and Soloviev (2004) is that the diurnal heating is not
 212 uniform, but will heat the relatively cold water more than the nearby warmer
 213 water, thereby masking existing temperature gradients. This may have a
 214 particular relevance to the fishing industry in coastal regions. Katsaros and
 215 Soloviev (2004) explained the effect of atmospheric regulation by the
 216 dependence of air-sea fluxes on the air-sea temperature difference. In our
 217 study we have shown that the dependence of the wind stress on the air-sea
 218 temperature difference also contributes to the atmospheric regulation of SST.
 219 The wind stress feedback is important mainly when the SST is originally
 220 below the air temperature, and increases during diurnal warming to a tem-
 221 perature above the air temperature.

Acknowledgments

223 We express our appreciation for the legacy that Joost Businger has left in
 224 air-sea interaction research. K. Katsaros acknowledges support by
 225 the National Oceanic and Atmospheric Administration, while she was at
 226 the Atlantic Oceanographic and Meteorological Laboratory in Miami at
 227 the beginning of this work and assistance by Ms. Gail Derr. The data on
 228 the Florida shelf were collected as a part of the NOVA Southeastern
 229 University and University of South Florida cooperative agreement under

230 ONR Grant N00014-98-1-0861 (via a subcontract to Florida Atlantic
231 University) and ONR Grant N00014-02-1-0950.

References

- 233 Bradley, E. F., Fairall, C. W., Hare, J. E., and Grachev, A. A.: 2000, 'An Old and Improved
234 Bulk Algorithm for Air-Sea Fluxes', in preprint, *14th Symposium on Boundary Layer and*
235 *Turbulence, Aspen, CO, August 7-11, 2000*, American Meteorological Society, 45 Beacon
236 St., Boston, MA, pp. 294-296.
- 237 Gentemann, C., Donlon, C. J., Stuart-Menteth, A., and Wentz, F. J.: 2003, 'Diurnal Signals in
238 Satellite Sea Surface Temperature Measurements', *Geophys. Res. Lett.* **30**(3), 1140-1143.
- 239 Katsaros, K. B., Fiuza, A., Sousa, F., and Amann, V.: 1983, 'Sea surface temperature patterns
240 and air-sea fluxes in the German Bight during MARSEN 1979, Phase I', *J. Geophys. Res.*
241 **88**, 9871-9882.
- 242 Katsaros, K. B. and Soloviev, A. V.: 2004, 'Vanishing Horizontal Sea Surface Temperature
243 Gradients at Low Wind Speeds', *Boundary-Layer Meteorol.* **112**(2), 381-396.
- 244 Mahrt, L., Vickers, D., and Moore, E.: 2004, 'Flow Adjustments across Sea-Surface Tem-
245 perature Changes', *Boundary-Layer Meteorol.* **111**(3), 553-564.
- 246 Soloviev, A. V. and Lukas, R.: 1997, 'Large Diurnal Warming Events in the Near-surface
247 Layer of the Western Equatorial Pacific Warm Pool', *Deep-Sea Res.* **44**, 1055-1076.
- 248 Soloviev, A., Walker, R., Weisberg, R., and Luther, M.: 2003a, 'Coastal Observatory
249 Investigates Energetic Current Oscillations on the Southeast Florida Shelf', *EOS, Trans-*
250 *actions, AGU* **84**(42), 441-450.
- 251 Soloviev, A. V., Luther, M. E., and Weisberg, R. H.: 2003b, 'Energetic baroclinic super-tidal
252 oscillations on the shelf off southeast Florida', *Geophys. Res. Lett.* **30**(9), 1463, doi: 10.1029/
253 2002GL016603.
- 254 Stramma, L., Cornillon, P., Weller, R. W., Price, J. F., and Briscoe, M. G.: 1986, 'Large
255 Diurnal Sea Surface Temperature Variability: Satellite and In-Situ Measurements', *J. Phys.*
256 *Oceanog.* **16**, 827-837.
- 257 Stuart-Menteth, A. C., Robinson, I. S., and Challenor, P. G.: 2003, 'A global Study of Diurnal
258 Warming using satellite-derived Sea Surface Temperature', *J. Geophys. Res.* **108** (C5),
259 3155, doi: 10.1029/2002JC001 534.
260